technologies

MDPI

Article

Effect of Particle Size on Microstructure and Mechanical Properties of Al-Based Composite Reinforced with 10 Vol.% Mechanically Alloyed Mg-7.4%Al Particles

Anil K. Chaubey [1,2,3], Prashanth Konda Gokuldoss [4,*], Zhi Wang [5], Sergio Scudino [6], Nilay K. Mukhopadhyay [3] and Jürgen Eckert [4,7]

1 Institute of Minerals and Materials Technology (IMMT), Bhubaneshwar 751013, India; anil.immt@gmail.com
2 Leibniz Institute for Solid State and Materials Research (IFW Dresden), Institute for Complex Materials, Postfach 270116, D-01171 Dresden, Germany
3 Department of Metallurgical Engineering, Indian Institute of Technology, Varanasi 221005, India; mukho.met@iitbhu.ac.in
4 Erich Schmid Institute of Materials Science, Austrian Academy of Sciences, Jahnstraße 12, A-8700 Leoben, Austria; juergen.eckert@oeaw.ac.at
5 School of Mechanical and Automotive Engineering, South China University of Technology, Guangzhou 510640, China; angw_zhi@sina.com
6 Solidification Processes and Complex Structures, Institute for Complex Materials, IFW Dresden, Helmholtzstraße 20, D-01069 Dresden, Germany; s.scudino@ifw-dresden.de
7 Department Materials Physics, Montanuniversität Leoben, Jahnstraße 12, A-8700 Leoben, Austria
* Correspondence: kgprashanth@gmail.com or Prashanth.kondagokuldoss@oeaw.ac.at; Tel.: +43-3842-804-206; Fax: +43-3482-804-116

Academic Editor: Anders E. W. Jarfors
Received: 20 August 2016; Accepted: 16 November 2016; Published: 19 November 2016

Abstract: The effect of Mg-7.4%Al reinforcement particle size on the microstructure and mechanical properties in pure Al matrix composites was investigated. The samples were prepared by hot consolidation using 10 vol.% reinforcement in different size ranges, D, $0 < D < 20$ μm (0–20 μm), $20 \leq D < 40$ μm (20–40 μm), $40 \leq D < 80$ μm (40–80 μm) and $80 \leq D < 100$ μm (80–100 μm). The result reveals that particle size has a strong influence on the yield strength, ultimate tensile strength and percentage elongation. As the particle size decreases from $80 \leq D < 100$ μm to $0 < D < 20$ μm, both tensile strength and ductility increases from 195 MPa to 295 MPa and 3% to 4% respectively, due to the reduced ligament size and particle fracturing. Wear test results also corroborate the size effect, where accelerated wear is observed in the composite samples reinforced with coarse particles.

Keywords: composite materials; particles size; consolidation; strength

1. Introduction

Al-based metal matrix composites (AMCs) are very attractive for lightweight applications such as aerospace, military and transport sectors due to high specific strength, good fatigue properties and wear resistance [1–5]. In addition, AMCs offer the possibility to tailor their properties to meet specific requirements [2–6]. The property of the AMCs depends on the property of the matrix and the reinforcement. Different types of reinforcement materials, ranging from typical ceramics, such as Al_2O_3, AlN and SiC [7–9], to more unconventional reinforcements, such as quasicrystals [10,11] and complex metallic alloys (CMAs) [12], have been successfully used as reinforcements in MMCs. Other possible candidates as reinforcing agents in MMCs are amorphous, partially amorphous and nanocrystalline Al-based alloys, which have attracted widespread attention as potential candidates for structural

as well as functional applications due to their high strength combined with low density [13,14]. Mg-7.4%Al alloy displays attractive properties, including low density (~1.79 g/cm^3), high room temperature strength (~700 MPa) and high hardness (170 Hv) [15]. Therefore, this phase is not only interesting in the monolithic form but it is also attractive as a potential candidate for reinforcement in lightweight high-strength MMCs.

AMCs can be processed by techniques like powder metallurgy/spray deposition/mechanical milling (MM) or by conventional casting. Powder metallurgy (PM) through solid-state sintering is widely used for the fabrication of such composites. It has excellent control over the microstructure of the composites, including size, morphology and volume fraction of the matrix and reinforcement [16,17]. In addition, PM is produced near net shape components at relatively low cost [18,19]. The properties of these composites depend strongly on the particle size and particle-matrix interface [20,21]. Reducing the particle size greatly improves the strength of these composites [22]. Accordingly, the present study focuses on the synthesis of Al-based composites using Mg-Al mechanically alloyed (MAed) powder as reinforcement and investigates the effect of particle size on the microstructure and mechanical properties of the composite at fixed reinforcement content.

2. Experimental Section

AMC reinforced with 10 vol.%MAed Mg-7.4Al (wt.%) particles were fabricated by mechanical milling, followed by hot consolidation. The reinforcement (Mg-7.4%Al mechanically alloyed particles) was prepared by mechanical alloying of elemental Mg (250 μm, Alfa Aesar, Karlsruhe, Germany) and Al (44 μm, Alfa Aesar) powders in a planetary ball mill for 100 h at room temperature followed by 3 h cryo-milling in liquid nitrogen. The detailed production and characterization of the reinforcement (Mg-7.4Al (wt.%)) has been reported elsewhere [23]. To study the effect of particle size, the composites were prepared with different particle sized reinforcement ($0 < D < 20$ μm (0–20 μm), $20 \leq D < 40$ μm (20–40 μm), $40 \leq D < 80$ μm (40–80 μm) and $80 \leq D < 100$ μm (80–100 μm)). MM was carried out using a Retsch PM400 planetary mill (Retsch, Haan, Germany) equipped with hardened steel balls and vials under Ar atmosphere for 3 h at 100 rpm with a ball-to-powder ratio of 10:1. All the sample handling was carried out in a glove box (mBraun, Garching, Germany) under purified argon atmosphere (<0.1 ppm O_2 and H_2O). The powders were then uni-axially hot pressed at 673 K and 400 MPa and subsequently hot-extruded at the same temperature with an extrusion ratio of 6:1. The as-extruded samples were machined into cylindrical tensile specimens of 3 mm diameter and 20 mm gauge length (as per ASTM E-8/E08M-08) [24]. Structural characterization of the samples was performed by X-ray diffraction (XRD) using a D3290 PANalyticalX'pert PRO with Co-Kα radiation (λ = 0.17889 nm) in Bragg-Brentano configuration (PANalytical, Kassel-Waldau, Germany). The *X*-ray was carried out in the step scanning mode, with tube voltage of 35 kV and tube current of 40 mA. A step size of 0.013 degree/min and a scanning rate of 1.5 degree/min was used for all measurements. Microstructural characterization was carried out by scanning electron microscopy (SEM) using a Gemini 1530 microscope (Jeol, München, Germany). The SEM images were taken in secondary electron mode at EHT voltage of 20 kV and aperture size of 60 μm. The density of the samples was evaluated using the Archimedes principle. The Vickers micro-hardness measurements were carried out using a computer-controlled Struers Duramin 5 Vickers hardness tester (Stuers, Willich, Germany). The device is equipped with a typical pyramidal diamond indenter with square base and an angle of 136° between the opposite faces. Indentations were carried out with an applied load of 0.01 kg and a dwell time of 10 s. The mechanical properties of the composites were evaluated under tensile loading using an Instron 5869 device (strain rate: 0.0017 s^{-1}) (INSTRON, Darmstadt, Germany). Wear experiments were conducted in the Pin-on-disc type Friction and Wear monitor (DUCOM; TL-20) (DUCOM, Bengaluru, India) with a data acquisition system against hardened ground steel disc (En-32) having hardness 65 HRC and surface roughness (Ra) 0.5 μm. The disc rotates. A load of 50 N was used for the wear experiments.

3. Results and Discussion

The XRD patterns of the pure Al, MAed Mg-7.4%Al powder and Al-based composites reinforced with 10 vol.% Mg-7.4%Al particles in different size range are presented in Figure 1a. The XRD pattern of the MAedMg-7.4% Al powder show the presence of MgAl solid solution ($MgAl_{(SS)}$) along with the intermetallic compound γ-$Al_{12}Mg_{17}$, which had formed during mechanical alloying. The patterns of the four composites with different particle sizes (Figure 1a) look identical due to same composition of the composites. The composite patterns show sharp fcc-Al peaks and small peaks of β-Al_3Mg_2 phase. The presence of β-Al_3Mg_2 phase reveals a possible phase transformation during the consolidation process. According to the phase diagram [25] pure Al and the Mg rich Al (Mg-7.4%Al particles) are not in equilibrium and the reaction between Al and the reinforcing Mg-7.4%Al particles can lead to the formation of the β-Al_3Mg_2 phase. In the present case, during hot consolidation at 673 K, atomic diffusion takes place, leading to the transformation of β-Al_3Mg_2 phase in the diffused region of Mg-7.4%Al particles.

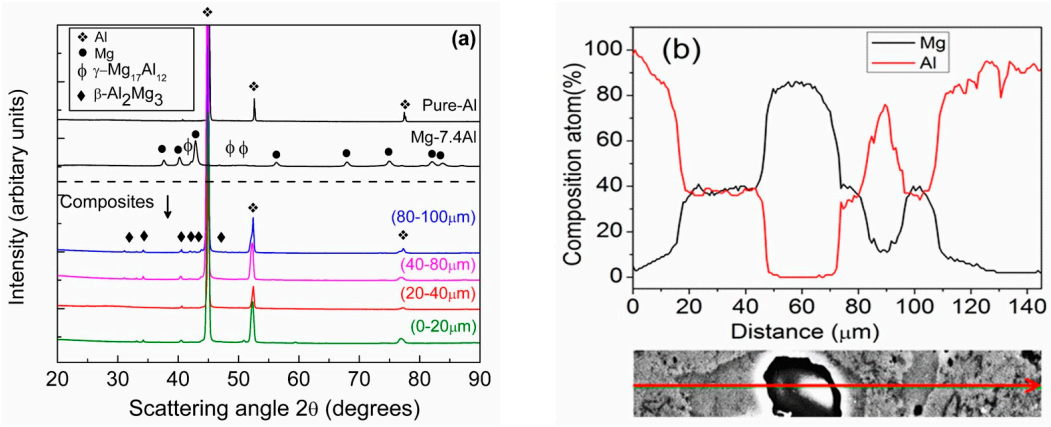

Figure 1. (**a**) *X*-ray diffraction (XRD) patterns for pure Al, mechanically alloyed Mg-7.4%Al powder and Al-based composites reinforced with different particle size; (**b**) compositional line profiles obtained from energy dispersive *X*-ray (EDX) analysis for the composite reinforced with (80–100 μm) particle size.

The SEM micrographs of the composites with (80–100 μm) particle size of the Mg-7.4%Al reinforcement (Figure 1b) display the presence of diffused regions around the reinforcement. The dark areas in Figure 1b are rich in Mg and the diffused regions (gray regions) constitute equiatomic Mg-Al that can be ascribed to the β-Al_3Mg_2 phase. The line scan also shows that the elemental distribution at the interfaces are not strictly steep, and ranges up to 10 μm, indicating physical mixing and/or atomic inter-diffusion at the Mg/Al interfaces leading to a strong interface bonding [26]. SEM micrographs of the composites (Figure 2a–d) reveal a homogeneous distribution of the reinforcement in the matrix. The micrograph (Figure 2a,b) shows three different areas in the sample, bright areas (matrix), semi-bright areas marked by circle (diffused area) and dark areas (Mg rich).

The micrographs of the composites reinforced with finer particles (Figure 2c,d) show only two different areas, bright (matrix) and dark (Mg rich areas) due to the smaller sized particles diffusing completely with the matrix. The density and hardness of the pure Al matrix along with the composite samples are shown in the Table 1. Since the reinforcement is lighter than the matrix, addition of the reinforcement decreases the density of the composite material, which is very clear from Table 1. The data also reveals that if the particle size of the reinforcement are decreased, the density as well as the hardness of the composite material increases, which may be due to the more compressibility and sinterablity of the finer particles with the matrix.

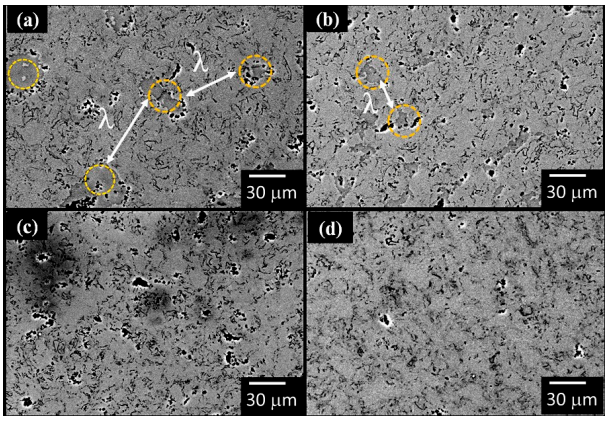

Figure 2. SEM micrographs for the consolidated composites with 10 vol.% of Mg-Al reinforcement with classified particle size (**a**) 80–100 μm; (**b**) 40–80 μm; (**c**) 20–40 μm and (**d**) 0–20 μm.

Table 1. Shows the density and hardness of the extruded samples.

Samples	Density (gm/cm^3)	Hardness (Hv)
Al pure	2.71 ± 0.15	42 ± 4
Al-10AlMg (80–100 μm)	2.61 ± 0.25	85 ± 7
Al-10AlMg (40–80 μm)	2.63 ± 0.24	87 ± 6
Al-10AlMg (20–40 μm)	2.64 ± 0.22	88 ± 5
Al-10AlMg (0–20 μm)	2.65 ± 0.18	89 ± 4

The tensile test results of the composites reinforced with different particle sizes are shown in Figure 3a. The result reveals that the strength of the composite increases with decrease in the particle size. It increases from 195 MPa for (80–100 μm) sized particles to 250 MPa for (40–80 μm) particles size, and finally to 295 MPa for $0-20$ μm sized samples with significant plastic deformation. Higher work hardening rate was observed with decreasing the particle size, which is attributed to the formation of dislocation tangles around the particles, due to plastic incompatibility between the reinforcement and matrix, and the formation of a dislocation cell structure with a cell size inversely proportional to the inter particle spacing [27–29]. The increase in strength of the material can be explained by using the Equation (1) [12]. At a constant amount of reinforcement, the distance between the particles (λ) decrease with decrease of particle size. Therefore, the number obstacles against the grain boundary movement increase with the particle size reduction, leading to a reduced grain boundary movement.

The inset in Figure 3a shows the dependence of the yield strength on $\lambda^{-1/2}$. The ligament size λ was measured from the microstructure of the composites (Figure 2), which reveals that the matrix ligament size λ increases from 15 to 20, 29 and 40 μm for the composite reinforced with powders of size (0–20 μm), (20–40 μm), (40–80 μm) and (80–100 μm) respectively. In other words, λ decreases with decreasing particle size of the reinforcement. The λ value also calculated using Equation (2) is proposed by Gustafson et al. [30], where λ is matrix ligament size, V volume fraction and D is the diameter of the particles. It is found that the calculated λ value and measured value are almost similar, hence corroborating our experimental results. Furthermore, the insert in Figure 3a shows a nearly linear relationship between yield strength and $\lambda^{-1/2}$, corroborating the validity of Equation (1), and demonstrates that the matrix ligament size has a significant role in strengthening the composites.

$$\Delta\sigma_s = k \cdot \lambda^{-1/2} \tag{1}$$

$$\lambda = D\left[\frac{1}{(V/100)^{1/3}} - 1\right] \tag{2}$$

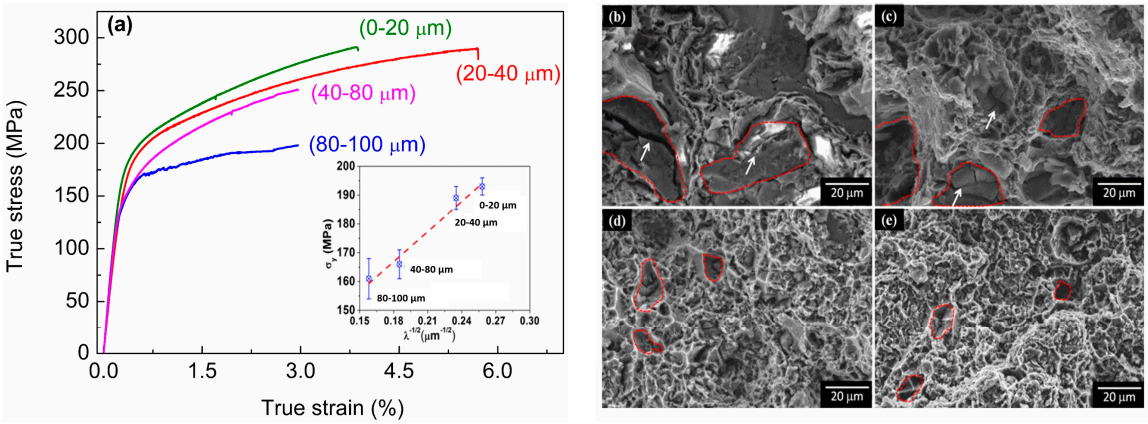

Figure 3. (**a**) Room temperature tensile true stress-true strain curves with inset showing the dependence of yield strength (σ_y) on $\lambda^{-1/2}$ and SEM micrographs of the fracture surface; (**b**) 80–100 μm; (**c**) 40–80 μm; (**d**) 20–40 μm and (**e**) 0–20 μm for the hot pressed and hot extruded composites with 10 vol.% of Mg-7.4%Alreinforcement.

Fracture surfaces of the reinforced composites (Figure 3b–d) reveal a clear contrast between the mode of fracture along the surface of the particles (brittle rupture) and the matrix (dimple rupture). The images (Figure 3b,c) of the composites reinforced with larger sized particles reveal several cracks (marked by arrow) because larger particles tend to crack easily [31].The particle/matrix interfaces remain intact, corroborating the proposal that the shear strength at the interface was higher than the particle fracture strength. Similar results have been also observed by Kumai et al. [32] in SiC particulate reinforced 6061 aluminum alloy. The composite reinforced with smaller size particles (Figure 3d,e) shows almost a ductile fracture with dimples embedded on the reinforcement.

Figure 4 presents the wear surface of the composites as a function of reinforcement particle size. The wear tracks of the composites show the presence of typical wear features including wear scars, ploughing grooves, and delamination. The composites with (80–100 μm) particle size show shallow ploughing grooves along with the presence of some delamination cracks (Figure 4a), which are formed at the surface of the sample in contact with the counter disc due to high strain levels developed during the wear test [33–35]. The samples of 40–80 μm particles size (seen in Figure 4b) also show a similar nature of wear surface but ploughing groves are not clearly visible. A further decrease in particle size (20–40 μm) of the reinforcement (Figure 4c) leads to the presence of smooth wear surface with small delamination near the wear track. Finally, the composite with reinforcement particles smaller than 20 μm shows smooth wear surface with a finer wear scar (Figure 4d). Figure 5 shows the wear data of the composites and it can be observed that, with increase in the particle size or the particle size range, the weight loss increases. In the other words, the wear rate increases with an increase in the particles size. The present results corroborate the tensile test results as well as the discussion held on the matrix ligament size, suggesting that reduction in particle size not only aids in improving the strength of the composite but also ductility.

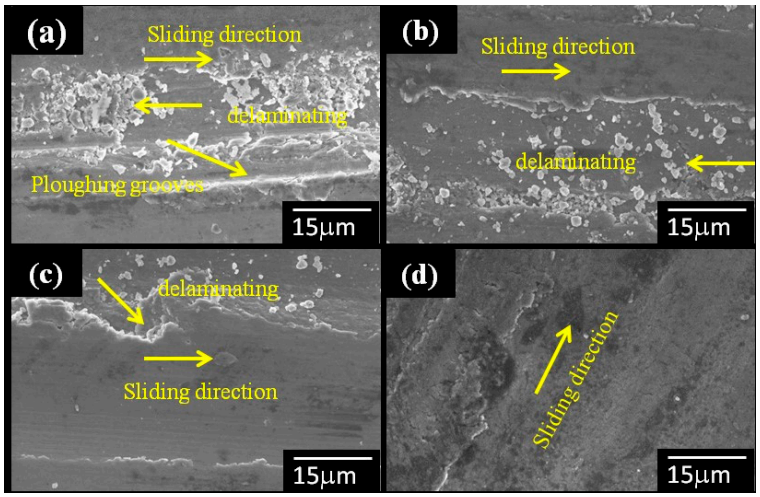

Figure 4. SEM micrographs showing the wear morphology of worn surfaces of composites reinforcement with classified particle size (**a**) 80–100 μm; (**b**) 40–80 μm; (**c**) 20–40 μm and (**d**) 0–20 μm.

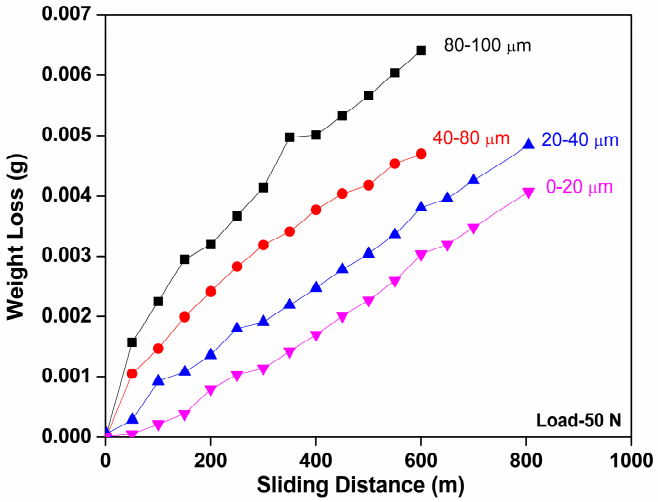

Figure 5. Pin-on-disc experiment showing the mass loss data as a function of sliding distance at a load of 50 N for the composites with different reinforcement size.

4. Conclusions

The effect of reinforcement particle size on the microstructure and mechanical property of the Al-(Mg-7.4%Al) composites was investigated. It can be summarized that (a) with a decrease in the particle size, the matrix ligament size decreases with a fairly uniform distribution of the reinforcement (b) the decrease in the size of the reinforcement increases the strength of the composite by around 50% (c) the yield strength of the composites has been modeled by taking into account matrix ligament size for the composites and the calculations are in very good agreement with the experimental results, revealing that the reduction of the matrix ligament size due to reduction in particle size acts as the main strengthening mechanism in these composites. This argument holds true with the wear properties of the composites as well.

Acknowledgments: The authors are grateful to Deutscher Akademischer Austausch Dienst (DAAD) Germany for providing the financial support to carry out this work.

Author Contributions: A.K.C, P.K.G., S.S. and J.E. conceived and designed the experiments; A.K.C. and Z.W. performed the experiments; A.K.C., K.G.P., N.K.M. and S.S. analyzed the data; K.G.P. and A.K.C. wrote the paper. J.E. supervised the research project.

Conflicts of Interest: The authors declare no conflict of interest.

References

1. Scudino, S.; Liu, G.; Prashanth, K.G.; Bartusch, B.; Surreddi, K.B.; Murty, B.S.; Eckert, J. Mechanical properties of Al-based metal matrix composites reinforced with Zr-based glassy particles produced by powder metallurgy. *Acta Mater.* **2009**, *57*, 2029–2039. [CrossRef]
2. Clyne, T.W.; Withers, P.J. *An Introduction to Metal Matrix Composites*; Cambridge University Press: New York, NY, USA, 1993.
3. Kainer, K.U. *Metal Matrix Composites. Custom-Made Materials for Automotive and Aerospace Engineering*; Wiley-VCH: Weinheim, Germany, 2006.
4. Wang, Z.; Prashanth, K.G.; Scudino, S.; Chaubey, A.K.; Sordelet, D.J.; Zhang, W.W.; Li, Y.Y.; Eckert, J. Tensile properties of Al matrix composites reinforced with in situ $Al_{84}Gd_6Ni_7Co_3$ glassy particles. *J. Alloy. Compd.* **2014**, *586*, S419–S422. [CrossRef]
5. Miracle, D.B. Metal matrix composites—From science to technological significance. *Compos. Sci. Technol.* **2005**, *65*, 2526–2540. [CrossRef]
6. Torralba, J.M.; Da Costa, C.E.; Velascoa, F. P/M aluminum matrix composites: An overview. *J. Mater. Process. Technol.* **2003**, *133*, 203–206. [CrossRef]
7. Liua, Y.Q.; Conga, H.T.; Wanga, W.; Sun, C.H.; Cheng, H.M. AlN nanoparticle-reinforced nanocrystalline Al matrix composites: Fabrication and mechanical properties. *Mater. Sci. Eng. A* **2009**, *505*, 151–156. [CrossRef]
8. Wang, H.Y.; Jiang, Q.C.; Wang, Y.; Ma, B.X.; Zhao, F. Fabrication of TiB_2 particulate reinforced magnesium matrix composites by powder metallurgy. *Mater. Lett.* **2004**, *58*, 3509–3513. [CrossRef]
9. Kanga, Y.C.; Lap-Ip Chan, S. Tensile properties of nanometric Al_2O_3 particulate-reinforced aluminum matrix composites. *Mater. Chem. Phys.* **2004**, *85*, 438–443. [CrossRef]
10. Schurack, F.; Eckert, J.; Schultz, L. Synthesis and mechanical properties of high strength aluminium-based quasicrystalline composites. *Philos. Mag.* **2003**, *83*, 1287–1305. [CrossRef]
11. El Kabir, T.; Joulain, A.; Gauthier, V.; Dubois, S.; Bonneville, J.; Bertheau, D. Hot isostatic pressing synthesis and mechanical properties of Al/Al–Cu–Fe composite materials. *J. Mater. Res.* **2008**, *23*, 904–910. [CrossRef]
12. Scudino, S.; Liu, G.; Sakaliyska, M.; Surreddi, K.B.; Eckert, J. Powder metallurgy of Al-based metal matrix composites reinforced with β-Al_3Mg_2 intermetallic particles: Analysis and modeling of mechanical properties. *Acta Mater.* **2009**, *57*, 4529–4538. [CrossRef]
13. Inoue, A. Amorphous: Nanoquasicrystalline and nanocrystalline alloys in Al-based systems. *Prog. Mater. Sci.* **1998**, *43*, 365–520. [CrossRef]
14. Inoue, A.; Kimura, H. Fabrications and mechanical properties of bulk amorphous, nanocrystalline, nanoquasicrystalline alloys in aluminum-based system. *J. Light Mater.* **2001**, *1*, 31–41. [CrossRef]
15. Chaubey, A.K.; Scudino, S.; Samadi Khoshkhoo, M.; Prashanth, K.G.; Mukhopadhyay, N.K.; Mishra, B.K.; Eckert, J. High-strength ultrafine grain Mg-7.4%Al alloy synthesized by consolidation of mechanically alloyed powders. *J. Alloy. Compd.* **2014**, *610*, 446–461. [CrossRef]
16. Omyma, E.-K.; Fathy, A. Effect of SiC particle size on the physical and mechanical properties of extruded Al matrix nanocomposites. *Mater. Des.* **2014**, *54*, 348–353.
17. Smagorinski, M.E.; Tsantrizos, P.G.; Grenier, S.; Cavasin, A.; Brzezinski, T.; Kim, G. The properties and microstructure of Al-based composites reinforced with ceramic particles. *Mater. Sci. Eng. A* **1998**, *244*, 86–90. [CrossRef]
18. Scudino, S.; Bartusch, B.; Eckert, J. Viscosity of the supercooled liquid in multi-component Zr-based metallic glasses. *J. Phys. Conf. Ser.* **2009**, *144*. [CrossRef]
19. Erich, D.L. Metal-matrix composites: Problems, applications and potential in P/M industry. *Prog. Powder Metall.* **1986**, *46*, 45–65.
20. Ali, F.; Scudino, S.; Liu, G.; Srivastava, V.C.; Mukhopadhyay, N.K.; Khoshkhoo, M.S.; Prashanth, K.G.; Uhlenwinkel, V.; Calin, M.; Eckert, J. Modeling the strengthening effect of Al-Cu-Fe quasicrystalline particles in Al-based metal matrix composites. *J. Alloy. Compd.* **2012**, *536*, S130–S133. [CrossRef]
21. Chaubey, A.K.; Scudino, S.; Mukhopadhyay, N.K.; Mishra, B.K.; Eckert, J. Effect of particle dispersion on the mechanical behavior of Al-based metal matrix composites reinforced with nanocrystalline Al-Caintermetallics. *J. Alloy. Compd.* **2012**, *536*, S134–S137. [CrossRef]

22. Slipenyuk, A.; Kuprin, V.; Milman, Yu.; Goncharuk, V.; Eckert, J. properties of P/M processed particle reinforced metal matrix composites specified by reinforcement concentration and matrix-to-reinforcement particle size ratio. *Acta Mater.* **2006**, *54*, 157–166. [CrossRef]
23. Chaubey, A.K.; Scudino, S.; Khoshkhoo, M.S.; Prashanth, K.G.; Mukhopadhyay, N.K.; Mishra, B.K.; Eckert, J. Synthesis and characterization of nanocrystalline Mg-7.4%Al powders produced by mechanical alloying. *Metals* **2013**, *3*, 58–68. [CrossRef]
24. ASTM-E8/E08M-08. *Standard Test Methods for Tension Testing of Metallic Materials*; ASTM International: West Conshohocken, PA, USA, 2008.
25. Alloy phase diagrams. In *ASM Handbook*; ASM International: Materials Park, OH, USA, 1997.
26. Standard terminology relating to methods of mechanical testing. In *ASTM Annual Book*; ASTM: West Conshohocken, PA, USA, 2003.
27. Manoharan, M.; Lewandowski, J.J. Effect of reinforcement size and matrix microstructure on the fracture properties of an aluminum metal matrix composite. *Mater. Sci. Eng. A* **1992**, *150*, 179–186. [CrossRef]
28. Lewandowski, J.J.; Liu, D.S.; Liu, C. Observations on the effects of particle size and superposed pressure in deformation of metal matrix composites. *Scr. Metall.* **1991**, *25*, 21–26. [CrossRef]
29. Kamat, S.; Hirth, J.P.; Mehrabian, R. Mechanical properties of particle-reinforced aluminum-matrix composites. *Acta Metall.* **1989**, *37*, 2395–2402. [CrossRef]
30. Gustafson, T.W.; Panda, P.C.; Song, G.; Raj, R. Influence of microstructural scale on plastic flow behavior of metal matrix composites. *Acta Mater.* **1997**, *45*, 1633–1643. [CrossRef]
31. Llorca, J. An analysis of the influence of reinforcement fracture on the strength of discontinuously-reinforced metal-matrix composites. *Acta Metall.* **1995**, *43*, 181–192. [CrossRef]
32. Kumai, S.; King, J.E.; Knott, J.F. Short and long fatigue crack growth in a SiC reinforced aluminium alloy. *Fatigue Fract. Eng. Mater. Struct.* **1990**, *13*, 511–524. [CrossRef]
33. Ehtemam-Haghighi, S.; Prashanth, K.G.; Attar, H.; Chaubey, A.K.; Cao, G.H.; Zhang, L.C. Evaluation of mechanical and wear properties of Ti-xNb-7Fe alloys designed for biomedical applications. *Mater. Des.* **2016**, *111*, 592–599.
34. Prashanth, K.G.; Debalina, B.; Wang, Z.; Gostin, P.F.; Gebert, A.; Calin, M.; Kühn, U.; Kamaraj, M.; Scudino, S.; Eckert, J. Tribological and corrosion properties of Al-12Si produced by selective laser melting. *J. Mater. Res.* **2014**, *29*, 2044–2054. [CrossRef]
35. Prashanth, K.G.; Scudino, S.; Chaubey, A.K.; Löber, L.; Wang, P.; Attar, H.; Schimansky, F.P.; Pyczak, F.; Eckert, J. Processing of Al–12Si–TNM composites by selective laser melting and evaluation of compressive and wear properties. *J. Mater. Res.* **2016**, *31*, 55–65. [CrossRef]